AD-A143 927 ON THE MODELING OF ELECTROMAGNETICALLY COUPLED MICROSTRIP ANTENNAS - THE. (U) CALIFORNIA UNIV LOS ANGELES INTEGRATED ELECTROMAGNETICS LAB 1/1

UNCLASSIFIED P B KATEHI ET AL. 30 APR 84 UCLA-ENG-84-12 F/G 9/5 NL

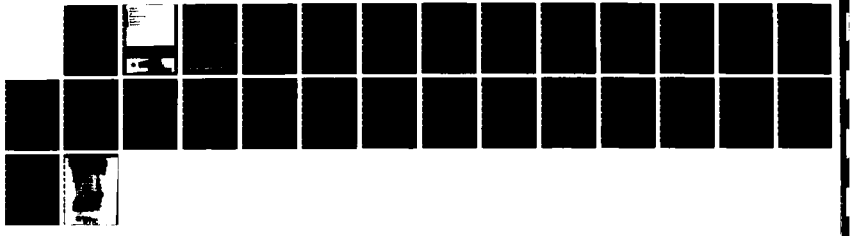

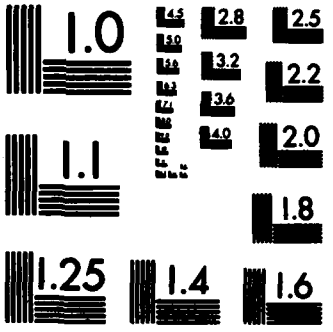

UCLA School of Engineering and Applied Science

"On the Modeling of Electromagnetically Coupled Microstrip Antennas - The Printed Strip Dipole"

By: P. B. Katehi and N. G. Alexopoulos

Integrated Electromagnetics Laboratory
Report No. 13
UCLA Report No. ENG-84-12
April 30, 1984

Sponsored by Research Contracts:
U.S. Army Contract DAAC 29-83-K-0067
U.S. Navy Contract N00014-79-C0856 Mod. P00005

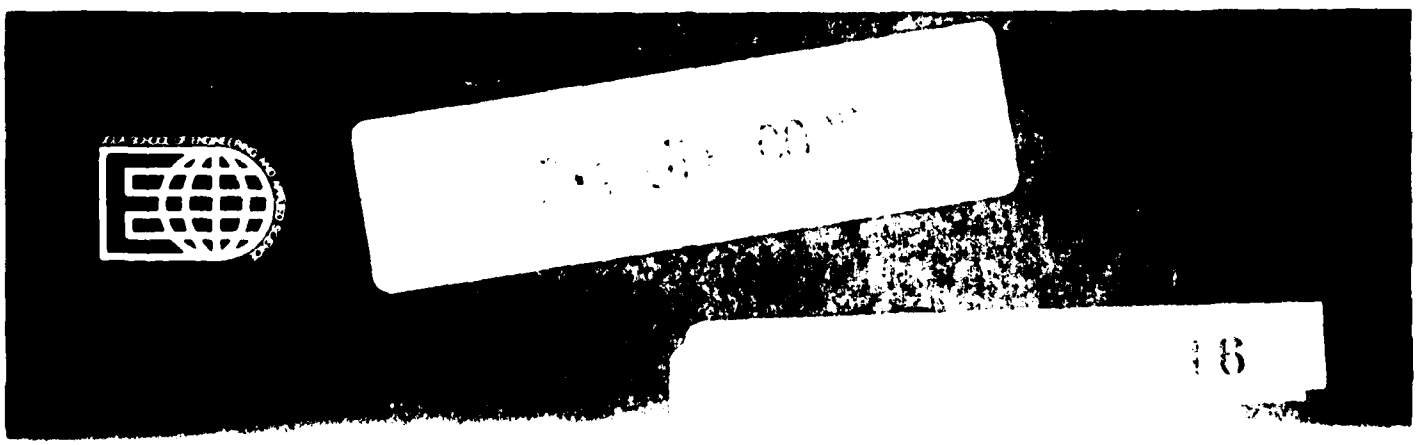

UNCLASSIFIED

SECURITY CLASSIFICATION OF THIS PAGE (When Data Entered)

REPORT DOCUMENTATION PAGE	READ INSTRUCTIONS BEFORE COMPLETING FORM
1. REPORT NUMBER ARO 19778.3-EL	2. GOVT ACCESSION NO. AD-A143927	3. RECIPIENT'S CATALOG NUMBER
4. TITLE (and Subtitle) "On the Modeling of Electromagnetically Coupled Microstrip Antennas-The Printed Strip Dipole"	5. TYPE OF REPORT & PERIOD COVERED
	6. PERFORMING ORG. REPORT NUMBER
7. AUTHOR(s) P. B. Katehi and N. G. Alexopoulos	8. CONTRACT OR GRANT NUMBER(s) U.S. Army DAAG 29-83-K-0067 U.S. Navy N00014-79-C0856 Mod. P00005.
9. PERFORMING ORGANIZATION NAME AND ADDRESS Electrical Engineering Department UCLA Los Angeles, CA 90024	10. PROGRAM ELEMENT, PROJECT, TASK AREA & WORK UNIT NUMBERS
11. CONTROLLING OFFICE NAME AND ADDRESS U. S. Army Research Office Post Office Box 12211 Research Triangle Park, NC 27709	12. REPORT DATE April 30, 1984
	13. NUMBER OF PAGES
14. MONITORING AGENCY NAME & ADDRESS(if different from Controlling Office) Army Research Office Research Triangle Park North Carolina / U.S. Navy Naval Weapon Center China Lake, CA	15. SECURITY CLASS. (of this report) Unclassified
	15a. DECLASSIFICATION/DOWNGRADING SCHEDULE

16. DISTRIBUTION STATEMENT (of this Report)

Approved for public release; distribution unlimited.

17. DISTRIBUTION STATEMENT (of the abstract entered in Block 20, if different from Report)

NA

AUG 3 1984

A

18. SUPPLEMENTARY NOTES

The view, opinions, and/or findings contained in this report are those of the author(s) and should not be construed as an official Department of the Army position, policy, or decision, unless so designated by other documentation.

19. KEY WORDS (Continue on reverse side if necessary and identify by block number)

20. ABSTRACT (Continue on reverse side if necessary and identify by block number)

A generalized solution for a class of printed circuit antennas, excited by a strip transmission line is presented. The strip transmission line may be embedded inside or printed on the substrate. As an example, microstrip dipoles electromagnetically coupled (parasitically excited) to embedded strip transmission line have been analyzed accurately and design graphs are provided for a specific substrate material. These graphs permit the establishment of a design procedure which yields the microstrip dipole length, overlap, offset, and substrate thickness with the goal of a desired input match for a given substrate material. The method accounts for conductor thickness and for arbitrary substrate parameters. Comparison with experiment shows excellent agreement.

DD FORM 1473 EDITION OF 1 NOV 65 IS OBSOLETE

UNCLASSIFIED

SECURITY CLASSIFICATION OF THIS PAGE (When Data Entered)

ON THE MODELING OF ELECTROMAGNETICALLY COUPLED MICROSTRIP ANTENNAS - THE PRINTED STRIP DIPOLE†

BY

P.B. Katehi and N. G. Alexopoulos
Electrical Engineering Department
University of California Los Angeles
Los Angeles, California 90024

A-1

†Performed under U.S. Army Research Contract DAAG 29-83-K-0067 and U.S. Navy Contract N00014-79-C0856 Mod. P00005.

ABSTRACT

A generalized solution for a class of printed circuit antennas, excited by a strip transmission line is presented. The strip transmission line may be embedded inside or printed on the substrate. As an example, microstrip dipoles electromagnetically coupled (parasitically excited) to embedded strip transmission line have been analyzed accurately and design graphs are provided for a specific substrate material. These graphs permit the establishment of a design procedure which yields the microstrip dipole length, overlap, offset, and substrate thickness with the goal of a desired input match for a given substrate material. The method accounts for conductor thickness and for arbitrary substrate parameters. Comparison with experiment shows excellent agreement.

I INTRODUCTION

This paper addresses the problem of rectangularly shaped and electromagnetically coupled printed circuit antennas. In this case, the excitation mechanism is provided by a strip transmission line embedded inside the substrate (see Figures 1, 2) which couples energy parasitically to the microstrip antenna. Electromagnetically coupled microstrip dipoles [1]-[5] have been investigated by empirical or approximate analysis techniques, and a very approximate model has been derived for the rectangular microstrip patch [6]. Since the radiation mechanism of a microstrip dipole is very similar to that of a microstrip patch [2], the model developed in this article is applicable to the analysis and design of microstrip elements which are rectangularly shaped but with a width smaller than the element length. Reference to Figures 1 and 2 assists in emphasizing that the parameters of the problem are arbitrary in the development of the model, including substrate thickness and relative permittivity to account for previously recognized substrate effects [7]-[15]. In addition, the thickness of metallic conductors is included, strip transmission line and microstrip antenna widths may differ and the effects of the microstrip antenna overlap and offset with respect to the transmission line on the current distribution is investigated. Finally, the model presented in this paper can resolve (see Figure 3), by the proper choice of parameters, the problems of the electromagnetically coupled rectangular microstrip patch antenna, the electromagnetically coupled microstrip dipole, the microstrip fed rectangular patch, radiation by an open circuited microstrip transmission line, as well as variations of these geometries.

The emphasis of this article is centered on the application of the theoretical model to electromagnetically coupled microstrip dipoles, comparison with published experimental results [5] and provision of design graphs for a specific substrate material. The model is developed by obtaining the current distribution along the dipole and transmission line, including all mutual

interactions. The Method of Moments is applied for the determination of the current distribution in the longitudinal dimension, while the current dependence in the transverse direction is chosen so as to satisfy the edge condition at the effective width location. Upon determining the current distribution, transmission line theory is invoked to evaluate at the chosen reference plane, the self impedance Z_g of the microstrip dipole. This leads to a design procedure which yields the microstrip dipole length, overlap and offset so that a desired input match can be achieved for a given substrate.

II. ANALYTICAL FORMULATION

A. Current Distribution Evaluation

The microstrip dipole and strip transmission line considered here have the cross sections shown in Figure 2. It is assumed that t_1 and t_2 are very small compared to wavelength in the dielectric ($t_1, t_2 \ll \lambda_g$). It is also assumed that the currents along the dipole and the feeding line flow on the bottom surfaces S_d and S_f. The electric field, under the assumption made, is given by Pocklington's Integral Equation

$$\vec{E}^i(\vec{r}) = \sum_{\nu=1,2} \iint_{ds_\nu} \overline{\overline{G}}_\nu^i(\vec{r}/\vec{r}') \cdot \vec{J}_\nu(\vec{r}')ds' \qquad (i = 1,2) \tag{1}$$

where $\vec{E}^i(\vec{r})$ is the electric field in medium i (i = 1 air, i = 2 dielectric) and $\overline{\overline{G}}_\nu^i(\vec{r}/\vec{r}')$ is the Dyadic Green's Function in medium i due to source ν (ν = 1 strip dipole, ν = 2 transmission line). The Dyadic Green's function is given by the expression

$$\overline{\overline{G}}_\nu^i(\vec{r}/\vec{r}') = [k_i^2\overline{\overline{I}} + \vec{\nabla}\vec{\nabla}] \cdot F_\nu^i(\vec{r}/\vec{r}') \tag{2}$$

$$\text{with } k_1 = \frac{2\pi}{\lambda_0} \text{ and } k_2 = \frac{2\pi}{\lambda_0}\sqrt{\varepsilon_r} \tag{3}$$

Since the widths of the dipole and microstrip line are fractions of the wavelength in the dielectric, it can be assumed that the currents are unidirectional and parallel to the x axis. Therefore, the current vector in Equation (1) can be written in the form

$$\vec{J}_\nu(\vec{r}') = \hat{x}\, J_x^\nu(x') J_y^\nu(y') \tag{4}$$

where $J_x^\nu(x')$ is an unknown function of x' while $J_y^\nu(y')$ is of the form

$$J_y^\nu(y') = \frac{2}{w_e^\nu \pi} \left\{ 1 - \left(\frac{2y'}{w_e^\nu} \right)^2 \right\}^{-1/2} \tag{5}$$

Here, w_e^ν is the effective strip width given by $w_e^\nu = w^\nu + 2\delta^\nu$. The parameter δ^ν is the excess half width and it accounts for fringing effects due to conductor thickness. Interpretation of the choice for the current density dependence in y', indicates that the edge condition is satisfied at $y' = \pm w_e^\nu/2$, which is an equivalent strip of zero thickness. At $y' = \pm \frac{w^\nu}{2}$, the current density remains finite, as is the case for nonzero thickness conductors. This choice of dependence in y' for the current density yields, as it will be shown very accurate results for microstrip dipole resonant length. Formulae for effective width exist in the literature [16], [17] and they have been adopted in this model formulation. The concept of effective width is thrust upon this formulation, since the current dependence in y' is assumed and not derived by numerical solution of Pocklington's Integral Equation in both the x and y directions. Equations (1) and (2) are combined now to yield ($ds' = dx'dy'$)

$$\vec{E}^i(\vec{r}) = \sum_{\nu=1,2} \int_0^{L_\nu} dx' \int_{-w^\nu/2}^{w^\nu/2} \frac{2}{w_e^\nu \pi} \left\{ 1 - \left(\frac{2y'}{w_e^\nu} \right)^2 \right\}^{-1/2} dy'$$

$$\left[k_1^2 \bar{\bar{I}} + \nabla\nabla \right] \cdot \bar{\bar{F}}_\nu^i(\vec{r}/\vec{r}') \cdot \hat{x}\, J_x^\nu(x') \tag{6}$$

with the dyadic $\overline{\overline{F}}^i_\nu(\vec{r}/\vec{r}')$ given by

$$\overline{\overline{F}}^i_\nu(\vec{r}/\vec{r}') = F^i_{\nu xx}(\vec{r}/\vec{r}')\,\hat{x}\hat{x} + F^i_{\nu zx}(\vec{r}/\vec{r}')\hat{z}\hat{x} \tag{7}$$

Substitution of (8) into (7) yields the following expression for the x component of the electric field:

$$E^i_x(r \sim \sum_{\nu=1,2} \int_0^{L_\nu} dx' \int_{w^\nu/2}^{w^\nu/2} \frac{dy'}{\left[1-\left(\frac{2y'}{w^\nu_e}\right)^2\right]^{1/2}} \left(\frac{2}{w^\nu_e \pi}\right)$$

$$\cdot\{k_1^2 F^i_{\nu xx} + \frac{\partial^2}{\partial x 2}(F^i_{\nu xx} - F^i_{\nu z})\} J^\nu_x(x') \tag{8}$$

where

$$F^i_{\nu xx} = 2\left(\frac{j\omega\mu_o}{4\pi k_1^2}\right) \int_o^\infty J_o(\lambda\rho)\, e^{-u_o t_1 \delta_{i1}} \cdot$$

$$\{1 - \delta_{i2}\,\delta_{\nu 2} + \delta_{i2}\,\delta_{\nu 2}[u\cosh(ub_s) + u_o \sinh(ub_s)]\} -$$

$$- \frac{\sinh[u(h-b'_s + b'_s\delta_{i1}\delta_{\nu 1})]}{f_1(\lambda,h)} \tag{9}$$

and $$F^i_{\nu z}(\vec{r}/\vec{r}') = -\int dx \left|\frac{\partial}{\partial z} F^i_{\nu zx}(\vec{r}/\vec{r}')\right| \tag{10}$$

with

$$F^i_{\nu z} = 2\left(\frac{j\omega\mu_o}{4\pi k_1^2}\right)(\epsilon_r - 1) \int_o^\infty J_o(\lambda\rho)\, e^{-u_o t_1 \delta_{i1}}$$

$$\frac{[\delta_{i1} u_o \cosh(uh) - \delta_{i2} u \sinh[u(h-b'_s)]}{f_1(\lambda,h)} \cdot$$

$$\frac{[\delta_{\nu 1}\sinh(uh) + \delta_{\nu 2}\sinh[u(h-b_s)]}{f_2(\lambda,\epsilon_r,h)} \tag{11}$$

Further definitions necessary for the interpretation of Equations (9) and (11) are provided as:

$$\delta_{ik} = \begin{cases} 1 & i = k \\ 0 & i \neq k \end{cases} = \text{Kronecker's delta}$$

$$\delta_{\nu k} = \begin{cases} 1 & \nu = k \\ 0 & \nu \neq k \end{cases} = \text{Kronecker's delta}$$

In addition,

$$b_s' = b_s - t_2 \ , \quad u_o = [\lambda^2 - k_1^2]^{1/2} \ , \quad u = [\lambda^2 - k_2^2]^{1/2}$$

$$f_1(\lambda,h) = u_o \sinh(uh) + u\cosh(uh) \tag{12}$$

$$f_2(\lambda,h) = \varepsilon_r u_o \cosh(uh) + u\sinh(uh) \tag{13}$$

and $$\rho = [(x-x')^2 + (y - y')^2]^{1/2} \tag{14}$$

The zeros of $f_1(\lambda,h)$ and $f_2(\lambda,h)$ lead to TE and TM surface wave modes respectively [7]-[15].

In order to solve Equation (8) for the currents $\vec{J}_1$ and $\vec{J}_2$, the method of moments is used. The strip dipole and fee line are divided into $N_\nu + 1$ segments with $\nu = 1,2$ respectively. The x' dependence of the current is written as

$$J_x^\nu(x') = \sum_{n=1}^{N_\nu} I_n^\nu f_n(x') \tag{15}$$

where the expansion functions $f_n(x')$ have been chosen to be piecewise sinusoidal functions given by

$$f_n(x') = \begin{cases} \dfrac{\sin[k(x' - x_{n-1})]}{\sin k\ell_x} & x_{n-1} \leq x' \leq x_n \\ \dfrac{\sin[k(x_{n+1} - x')]}{\sin k\ell_x} & x_n \leq x' \leq x_{n+1} \\ 0 & \text{anywhere else} \end{cases} \tag{16}$$

with ℓ_x the length of each subsection. By substituting Equation (15) into (8), the electric field can be written as

$$E_x^i(\vec{r}) = \sum_{\nu=1,2} \sum_{n=1}^{N_\nu} I_n^\nu \int_{-w^\nu/2}^{w^\nu/2} \frac{dy'}{\left[1 - \left(\frac{2y'}{w_e^\nu}\right)^2\right]^{1/2}} \left(\frac{2}{w_e^\nu \pi}\right)$$

$$\int_o^{L_\nu} dx' \left| k_i^2 F_{\nu xx}^i + \frac{\partial^2}{\partial x^2} (F_{\nu xx}^i - F_{\nu z}^i) \right| f_n(x') \qquad (17)$$

Furthermore, the electric field is projected along the x axis ($y = y^i$, $z = z^i$, $i = 1,2$) using as weighting functions the basis functions (Galerkin's Method) and therefore, Equation (17) reduces to a matrix equation of the form

$$[Z_{mn}^{i\nu}] \; [I_n^\nu] = [V_m^i] \quad ; \quad i = 1,2 \quad , \; \nu = 1,2 \qquad (18)$$

where $[V_m^i]$ is the excitation vector of order $N_1 + N_2$, $[I_n^\nu]$ is the vector of unknown coefficients of order $N_1 + N_2$ and $[Z_{mn}^{i\nu}]$ is the impedance matrix of order $(N_1 + N_2) \times (N_1 + N_2)$ whose elements are given by

$$Z_{mn}^{i\nu} = \delta(y - y^i) \; \delta(z - z^i) \int_{-w^\nu/2}^{w^\nu/2} \frac{dy'}{\left[1 - \left(\frac{2y'}{w_e^\nu}\right)^2\right]^{1/2}}$$

$$\int_o^{L_\nu} dx \int_o^{L_\nu} dx' \left| k_i^2 F_{\nu xx}^i + \frac{\partial^2}{\partial x^2} (F_{\nu xx}^i - F_{\nu z}^i) \right| f_m(x) f_n(x') \qquad (19)$$

Using this form for the evaluation of the elements of the impedance matrix, one can solve the matrix equation shown in (8) to find the unknown coefficients for the current.

B. Self-Impedance Evaluation

For the evaluation of the microstrip dipole self impedance, transmission line theory is applied and, because of this, unimodal behavior of the field far from the strip/dipole coupling region is essential. In order to satisfy this requirement, the transmission line is kept very close to the ground plane giving a ratio width/line-to-ground distance > 2.0.

For the particular geometry considered here, a unimodal field is excited under the transmission line and as a result the current distribution beyond an appropriate reference plane forms standing waves of a TEM-like mode. For this reason, the microstrip line is approximated by an ideal transmission line of characteristic impedance Z_o which is terminated to an unknown impedance Z_s (see Figure 4). This Quasi-TEM mode has a wavenumber β and a standing wave ratio SWR equal to the average values evaluated from the original current.

If the origin of x coordinate is taken at the position of Z_s, then the voltage and current waves on the ideal transmission line, with respect to this plane of reference, are given by:

$$V(x) = Ae^{-j\beta x} + Be^{j\beta x} \tag{20a}$$

and

$$I(x) = \frac{1}{Z_o}\left[Ae^{-j\beta x} - Be^{j\beta x}\right] \quad . \tag{20b}$$

Considering the positions x_{max} and x_{min} of two consecutive maxima and minima, Equation (20a) gives

$$\frac{I_{max}}{I_{min}} = \frac{1 - \frac{B}{A}e^{j2\beta x_{max}}}{1 - \frac{B}{A}e^{j2\beta x_{min}}} e^{-j\beta(x_{max} - x_{min})} \tag{21}$$

Since the absolute difference between x_{max} and x_{min} is equal to one-fourth of the wavelength of the guided wave ($x_{max} - x_{min} = \lambda_g/4$), then Equation (21) can be written as

$$\frac{I_{max}}{I_{min}} = \frac{1 - \frac{B}{A}e^{j2\beta x_{max}}}{1 - \frac{B}{A}e^{j2\beta x_{min}}} e^{\pm j\frac{\pi}{2}} \tag{22}$$

The reflection coefficient Γ is defined as

$$\Gamma(x) = \frac{B}{A}e^{j2\beta x} = \Gamma(0)\ e^{j2\beta x} \tag{23}$$

and by considering

$$\gamma = \frac{I_{max}}{I_{min}} e^{\pm j\frac{\pi}{2}} \tag{24}$$

then Equation (22) gives the following expression for the reflection coefficient,

$$\Gamma(o) = - \frac{\gamma - 1}{\gamma + 1} e^{-j2\beta x_{max}} \tag{25}$$

From (20a) and (20b) an expression for the self impedance Z_s evaluated at the position x_o can be written as follows:

$$\frac{Z_s(x_o)}{Z_o} = \frac{1 + \Gamma(x_o)}{1 - \Gamma(x_o)} \tag{26}$$

If now this plane of reference is considered at the position of the first current maximum d_{max} from the end of the open circuited transmission line, then the self impedance measured with respect to this plane is given by

$$\begin{aligned} \frac{Z_s(d_{max})}{Z_o} &= \frac{1 + \Gamma(d_{max})}{1 - \Gamma(d_{max})} \\ &= \frac{1 + \Gamma(0)e^{j2\beta d_{max}}}{1 - \Gamma(0)e^{j2\beta d_{max}}} \end{aligned} \tag{27}$$

Since for the evaluation of $\Gamma(d_{max})$, method of moments together with transmission line theory has been applied, Equation (27) indicates that the evaluated self-impedance depends on the characteristics of the substrate (ε_r,h) as well as on the embedding distance of the transmission line, the overlap, the offset and the length of the dipole.

The fundamental design procedure is now revealed. One wants to choose, for a given substrate, the right position of the dipole so that optimum resonance or in other words perfect match is obtained. The condition of optimum resonance is characterized by the relation

$$\frac{Z_s(d_{max})}{Z_o} = 1 \tag{28}$$

which combined with (27) gives

$$\Gamma(d_{max}) = 0 \tag{29}$$

or

$$\Gamma(x) = 0 \tag{30}$$

This means that one wishes to find the geometry which perfectly matches the dipole to the transmission line.

C. Numerical Results

The self impedance is evaluated using Equation (27) as a function of the length L_d of the dipole and the overlap κ_{ovp}

$$\kappa_{ovp} = \frac{S_1'}{S_1} \% \tag{31}$$

where S_i' is the part of the surface S_d of the dipole which is over the transmission line (Fig. 4). The real and imaginary parts of the normalized self impedance are plotted (Fig. 5) for a substrate thickness h = 0.077", dielectric constant $\varepsilon_r = 2.53$ and embedding distance $b_s = 0.0485"$. The width of the strips is w = 0.060" and the thickness t = 0.00025". The length of the dipole is varying between 0.373" and 0.349" and the overlap takes values between 38% and 86%. Figure 5 implies that there existsa particular overlap for which the curve of the dipole lengths goes through the point $\frac{Z_s}{Z_o} = 1$ or in other words, for the geometry considered above there is one value for the overlap and a specific dipole length so that the dipole is perfectly matched to the transmission line.

It is of interest to investigate now the dependence of the normalized self-impedance on the offset and the dipole length. For the geometry used previously, the overlap is kept at 50% while the dipole length is varying between 0.373" and 0.349" and the offset takes the values 0.00", 0.02", 0.04" and 0.08". From Figure 6, one can see that there is a specific offset for which the curve of the dipole lengths crosses the axis of the normalized self resistance at the point 1. Therefore, for this value of the offset, there is a dipole length which can give perfect match.

However, as it was mentioned before, the normalized self impedance is also a function of the substrate characteristics and the position of the transmission line. In order to examine this dependence, the dielectric constant, width, thickness, overlap and the distance of the transmission line from the ground plane are kept constant to the values above, while the dipole length is varied again between 0.373" and 0.349", and the embedding distance takes the values 0.036", 0.048", 0.054" and 0.066". Figure 7 indicates that there is a unique value for the embedding distance which combined with the appropriate dipole length can give perfect match.

It is also very interesting to see how the current distribution changes as a function of the embedding distance b_s around optimum resonance. Figure 8 displays the current distribution normalized to the incident current on the transmission line for h = 0.099" (undercoupled), h = 0.093" (perfectly matched and h = 0.082" (overcoupled). The substrate is duroid (ε_r = 2.53), the distance of transmission line to the ground plane is 0.0285" and the length of the dipole L_1 = 0.353". As it is shown in the figure the current on the dipole takes its maximum value when it is perfectly matched.

D. Comparison with Experimental Results

The theoretical analysis of a printed strip dipole electromagnetically coupled to an embedded microstrip line is tested by comparing theoretical results to experimental ones. Stern and Elliott [5] measured experimentally the self impedance of strip dipoles with rounded corners (Fig. 9) printed on duroid boards (ε_r = 2.35) with substrate thickness h = 0.077" and excited by a microstrip transmission line in the dielectric at a distance from the ground plane equal to 0.0285". The width of the strips is w = 0.06" and the thickness t = 0.00025". The self impedance was measured for different dipole lengths and its normalized values are shown on a Smith's chart (triangles) in Fig. 9. The solid line corresponds to the theoretical result. If one defines as resonant

length L_r the length of the dipole which gives a pure real self impedance, then the experimental resonant length is about 0.390" while the theoretical one 0.379". Therefore, there is a difference 2.75% with approximately 2% resulting from the different shape of the dipoles which were studied analytically (rectangular strips) and measured experimentally (strips with round corners) [18]. The difference between the theoretical and experimental values of the self impedance is due to two reasons: i) different shape of the dipoles, ii) the fact that in the theoretical evaluation of the current, the hybrid nature of the modes propagating in the microstrip was taken into account while for the experiments only an equivalent TEM mode was measured.

III. CONCLUSIONS

An effective method has been presented for the accurate modeling of rectangularly shaped printed circuit antennas which are excited parasitically by a strip transmission line embedded in the substrate. The various parameters involved, such as microstrip antenna and transmission line dimensions and location as well as substrate permittivity and thickness, are completely arbitrary in the model. The current distribution is computed by the method of moments in the longitudinal direction of the antenna and the transmission line, while in the transverse direction it is chosen as the Maxwell distribution, thus satisfying the edge condition at the printed element effective width. Comparison with experiment indicates that this model provides excellent accuracy.

FIGURES

REFERENCES

[1] H. G. Oltman, "Electromagnetically Coupled Microstrip Dipole Antenna Elements," in 8th European Microwave Conf., Paris, France, Sept. 1978.

[2] D. A. Huebner, "An Electrically Small Microstrip Dipole Planar Array," in Workshop Printed Circuit Antenna Technol., New Mexico State University, Las Cruces, NM, Oct. 1979.

[3] H. G. Oltman and D. A. Huebner, "Electromagnetically Coupled Microstrip Dipoles," IEEE Trans. Antennas Propagat., Vol. AP-29, pp. 151-157, Jan. 1981.

[4] R. S. Elliott and G. J. Stern, "The Design of Microstrip Dipole Arrays including Mutual Coupling, Part I: Theory," IEEE Trans. Antennas Propagat., Vol. AP-29, pp. 757-760, Sept. 1981.

[5] G. J. Stern and R. S. Elliott, "The Design of Microstrip Dipole Arrays including Mutual Coupling, Part II: Experiment," IEEE Trans. Antennas Propagat., Vol. AP-29, pp. 761-765, Sept. 1981.

[6] J. Rivera and T. Itoh, "Analysis of a Suspended Patch Antenna Excited by an Inverted Microstrip Line," Electromagnetics, Special Issue on Integrated Circuit Antennas (to be published).

[7] N. K. Uzunoglu, N. G. Alexopoulos, and J. G. Fikioris, "Radiation Properties of Microstrip Dipoles," IEEE Trans. Antennas Propagat., Vol. AP-27, pp. 853-858, Nov. 1979.

[8] I. E. Rana and N. G. Alexopoulos, "Current Distribution and Input Impedance of Printed Dipoles," IEEE Trans. Antennas Propagat., Vol AP-29, pp. 99-105, Jan. 1981.

[9] N. G. Alexopoulos and I. E. Rana, "Mutual Impedance Computation Between Printed Dipoles," IEEE Trans. Antennas Propagat., Vol. AP-29, pp. 106-111, Jan. 1981.

[10] N. G. Alexopoulos and I. E. Rana, "Current Distribution and Input Impedance of Printed Dipoles," Correction, IEEE Trans. Antennas Propagat., Vol. AP-30, pp. 822, July, 1982.

[11] P. B. Katehi and N. G. Alexopoulos, "On the Effect of Substrate Thickness and Permittivity on Printed Circuit Dipole Properties," IEEE Trans. Antennas and Propagation, Vol. AP-30, January, 1983.

[12] P. B. Katehi and N. G. Alexopoulos, "Real Axis Integration of Sommerfeld Integrals with Applications to Printee Circuit Antennas," J. Math. Phys. 24(3), March 1983.

[13] N. G. Alexopoulos, P. B. Katehi, and D. B. Rutledge, "Substrate Optimization for Integrated Circuit Antennas," IEEE Trans. on MTT, Vol. 31, No. 7, July 1983.

[14] D. M. Pozar, "Input Impedance and Mutual Coupling of Rectangular Microstrip Antennas," IEEE Trans. Antennas and Propagat., Vol. AP-30, pp. 1191-1196, No. 1982.

[15] D. M. Pozar, "Considerations for Millimeter Wave Printed Antennas," IEEE Trans. Antennas and Propagat., Vol. AP-31, pp. 740-747, September, 1983.

[16] K. C. Gupta, R. Garg, and I. J. Bahl, Microstrip Lines and Slotlines, Artech House, Inc., Dedham, Massachusetts, U.S.A., 1979.

[17] T. C. Edwards, Foundations for Microstrip Circuit Design, John Wiley and Sons Ltd., New York, 1981.

Acknowledgments. The authors wish to thank Professor R. S. Elliott for his helpful comments and encouragement. Also appreciation is due to Ms. I. Andreadis for typing the manuscript.

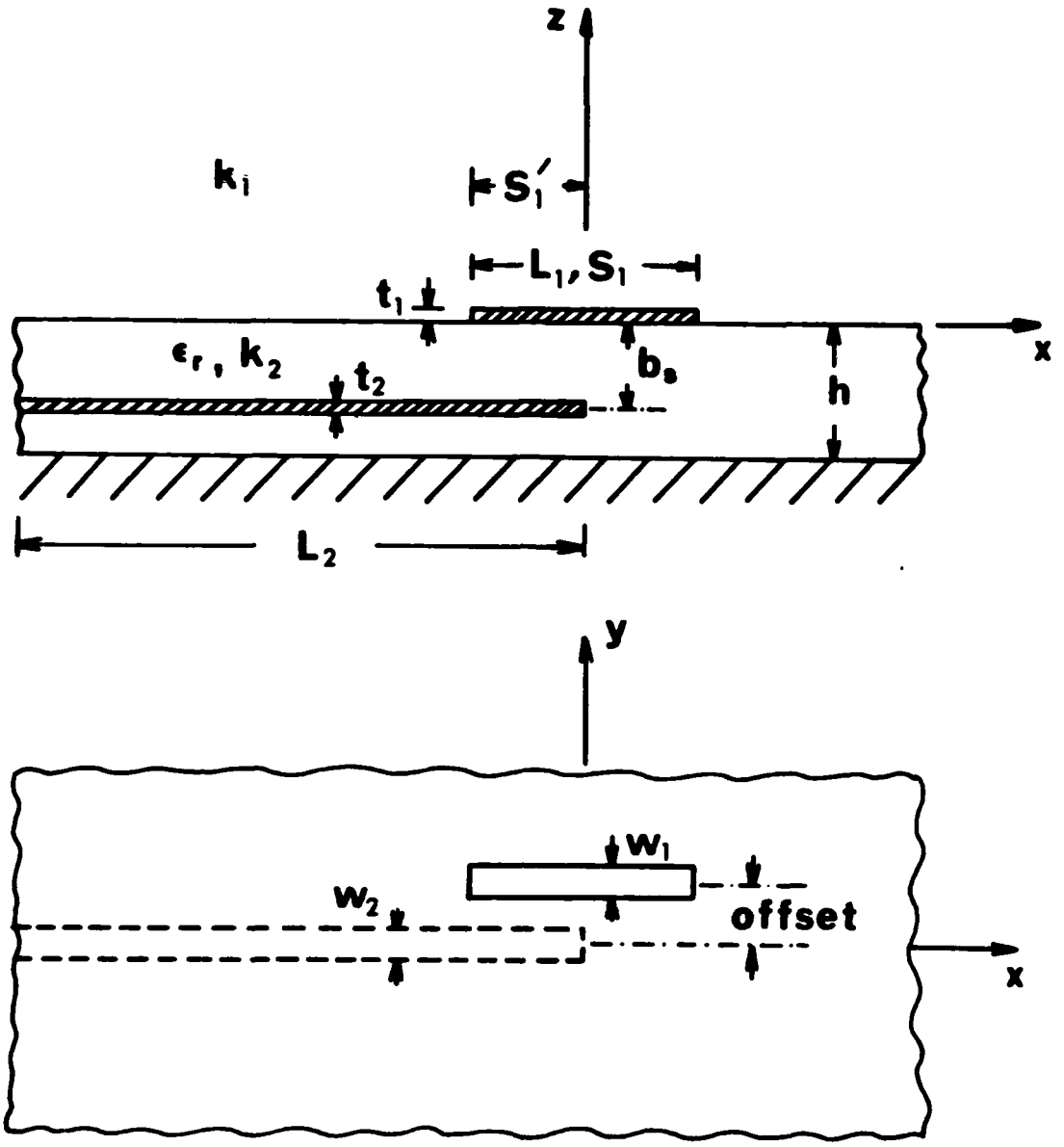

Figure 1

Side and top view of a printed strip dipole excited by a transmission line embedded in the dielectric.

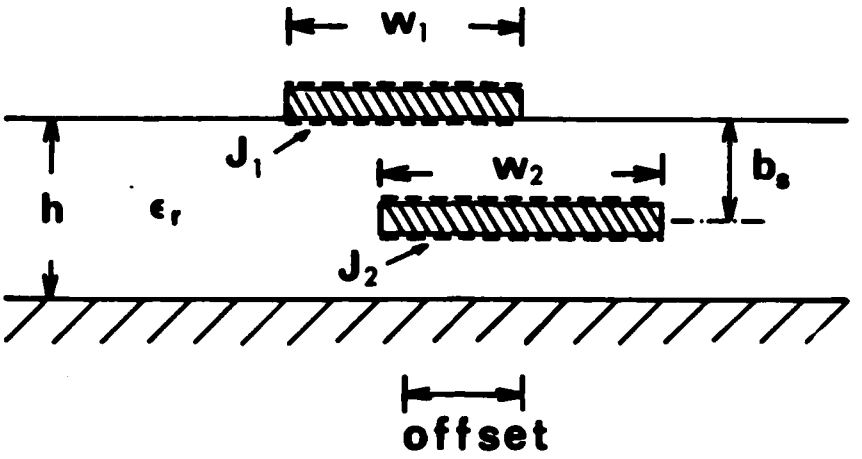

Figure 2

Cross section of a printed strip dipole excited by a transmission line embedded in the dielectric

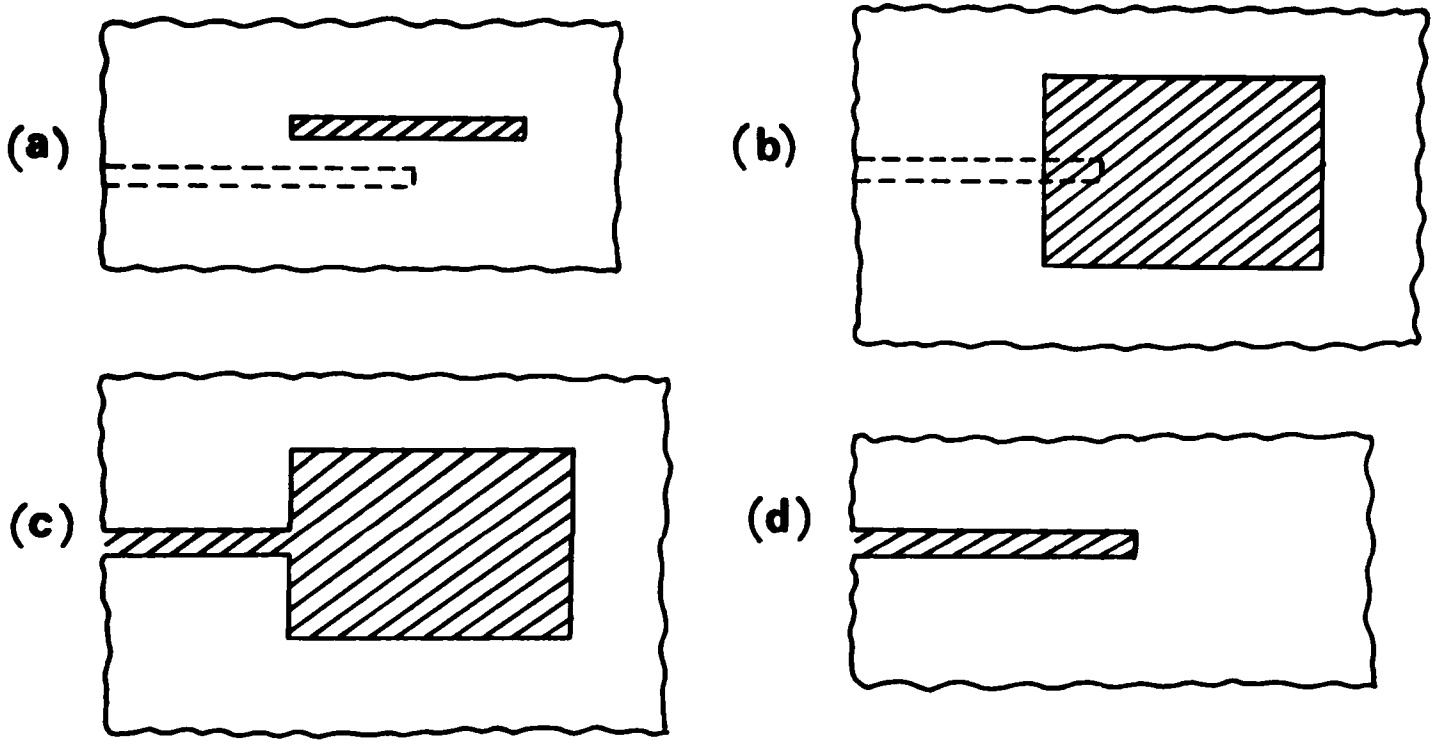

Figure 3

Some microstrip antenna geometries resolvable by proposed model

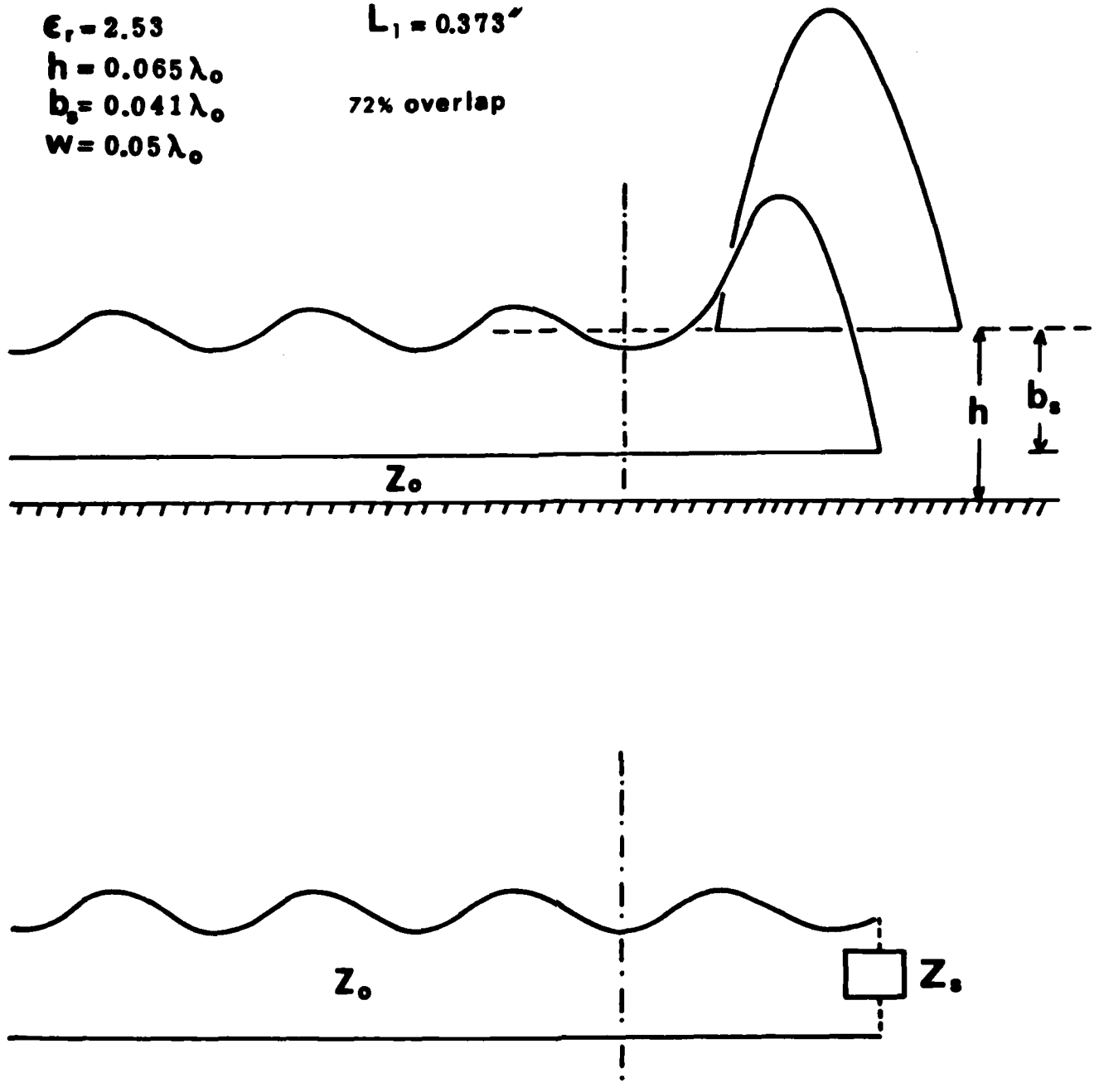

Figure 4

Current amplitude on the strip dipole and microstrip transmission line.

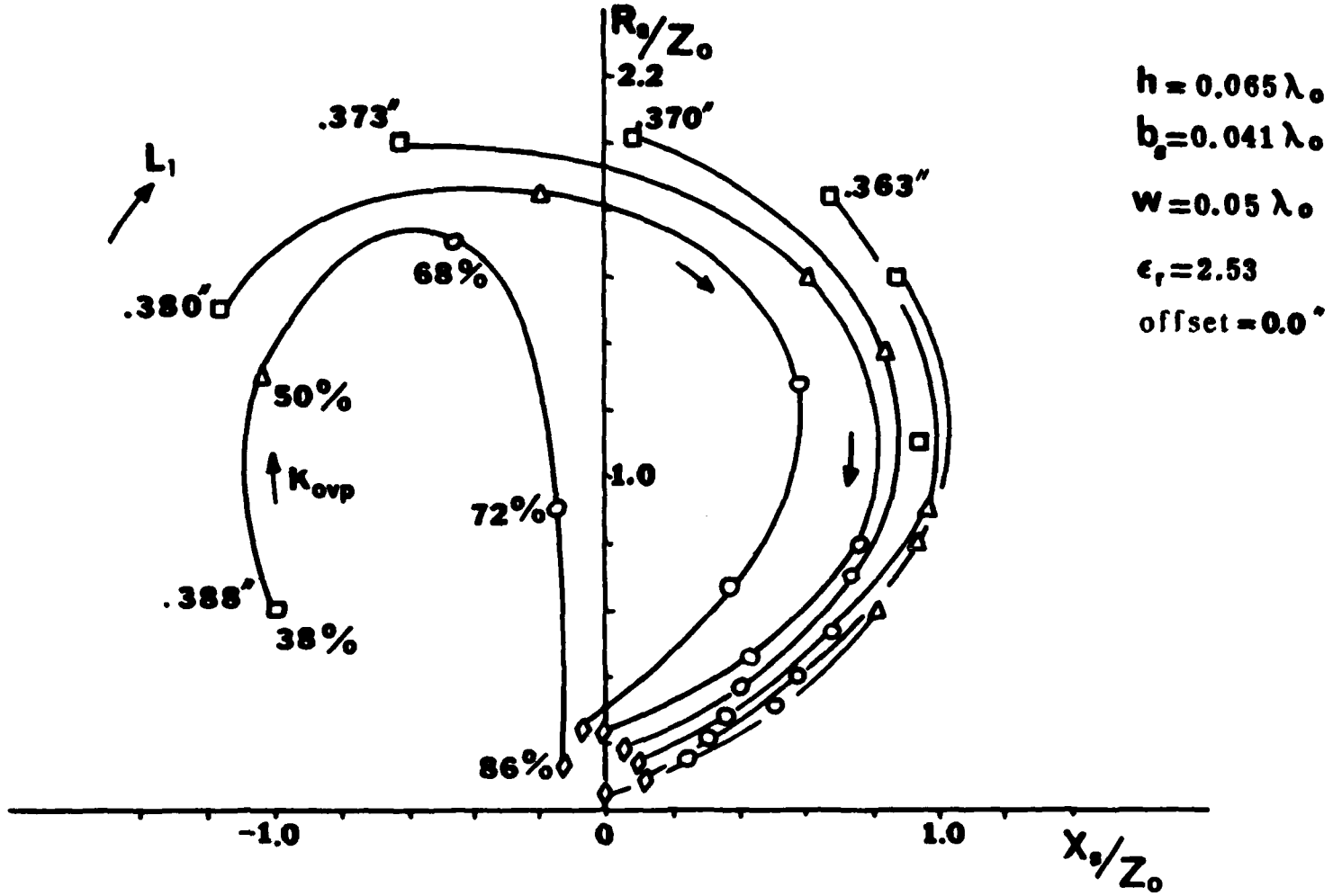

Figure 5

Z_s/Z_o as a function of k_{ovp} and L_1

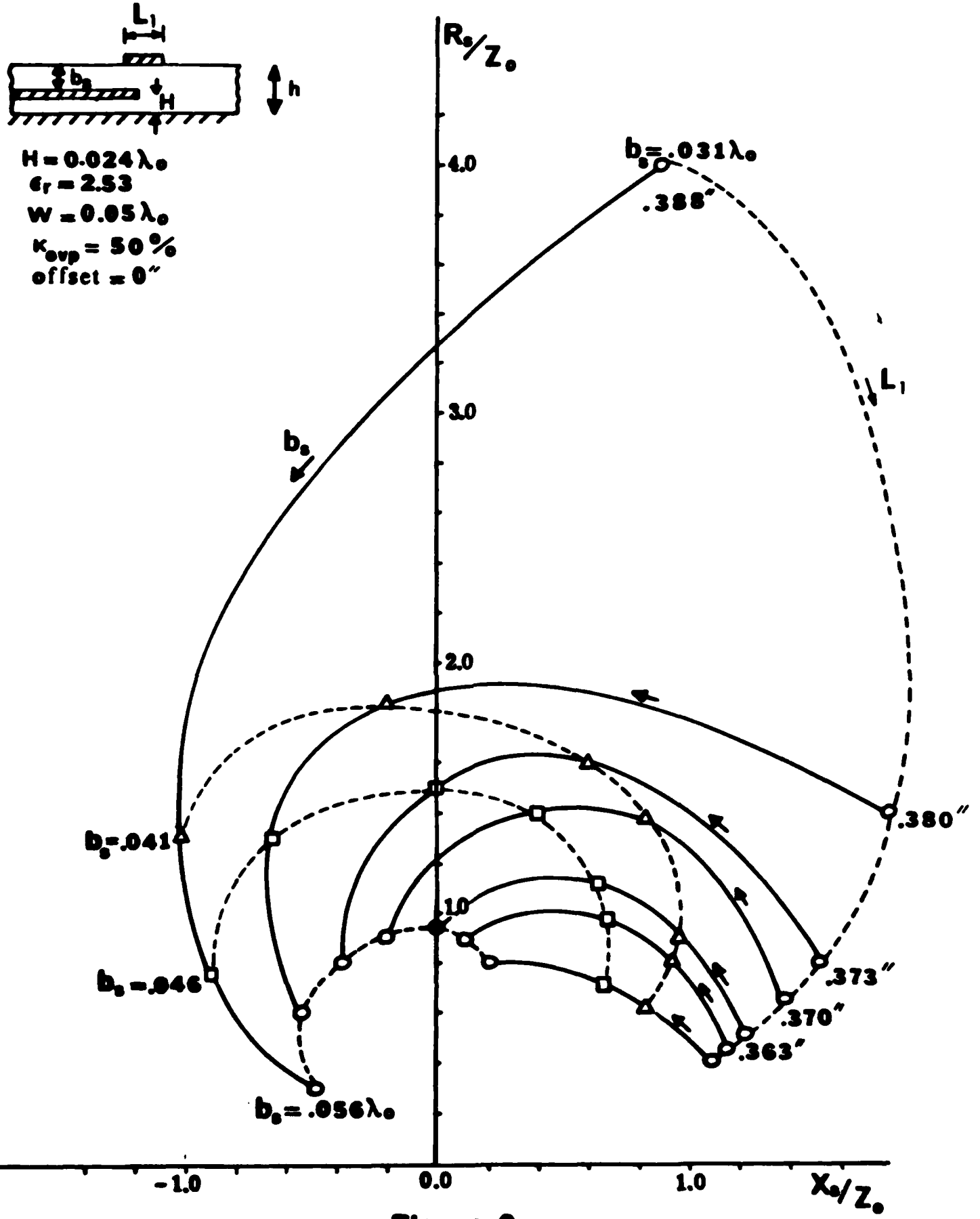

Figure 6

Z_0/Z_0 as a function of b_0 and L_1

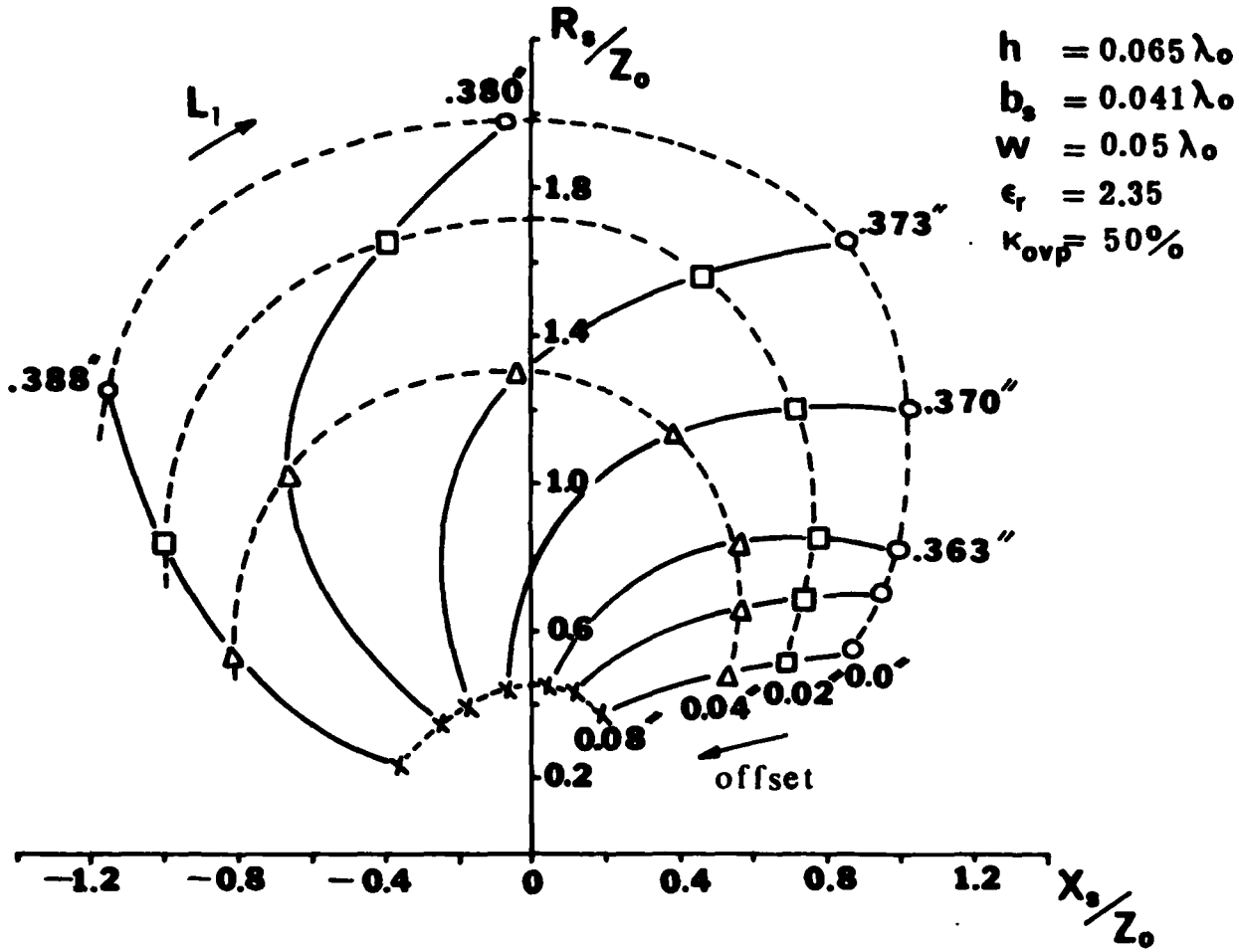

Figure 7

Z_s/Z_o as a function of the offset and L_1

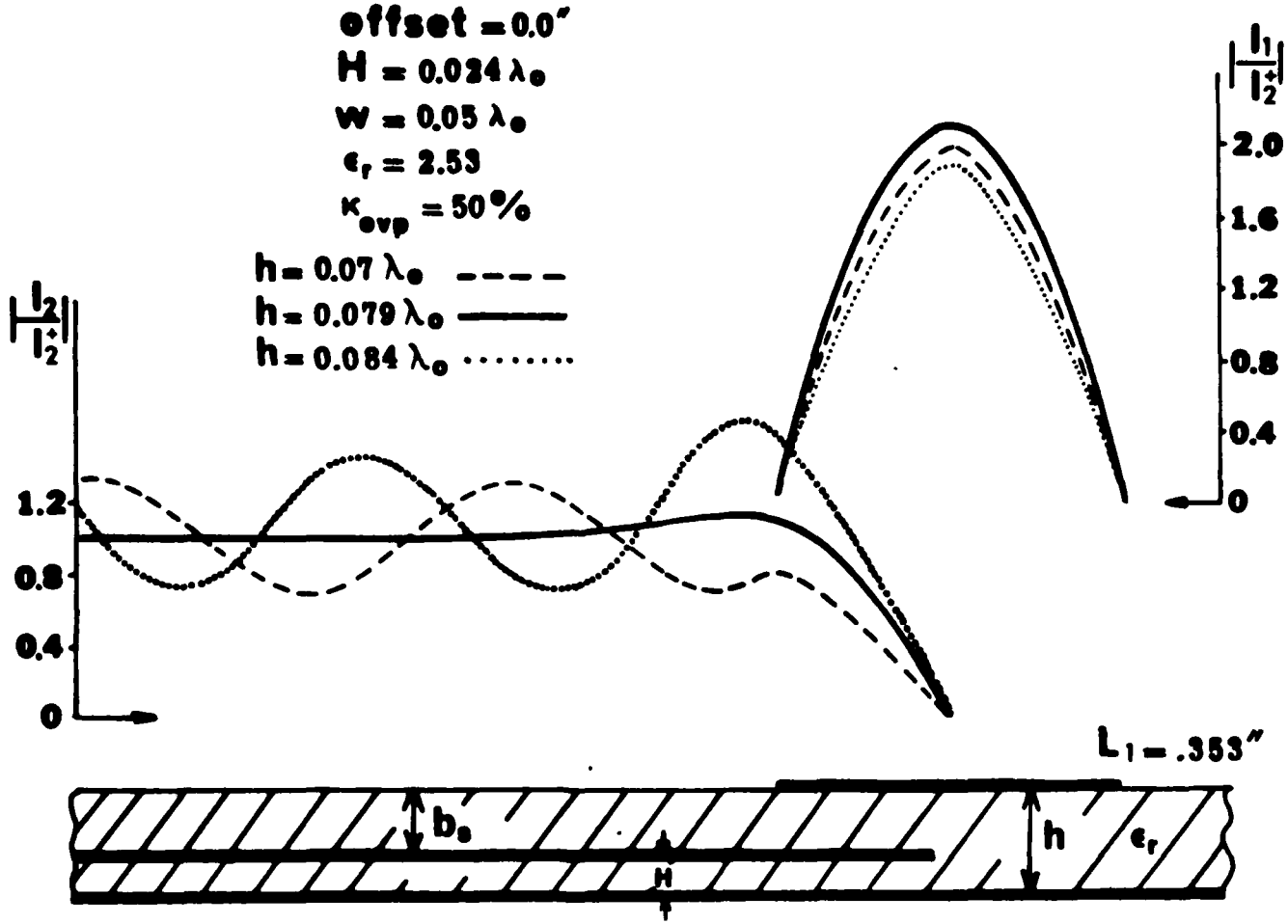

Figure 8

Current amplitude on the strip dipole and transmission line.

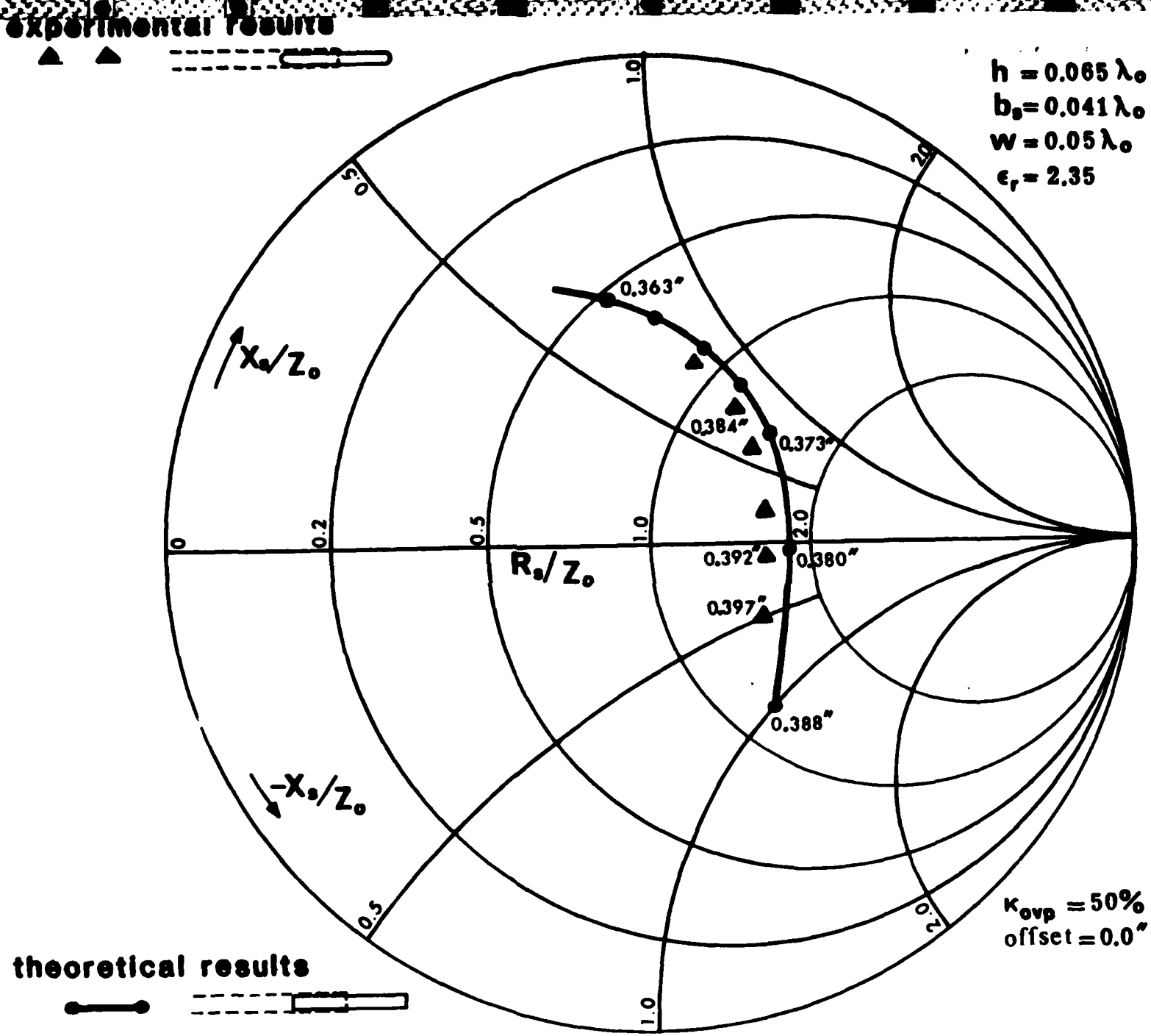

Figure 9 Comparison of theoretical to experimental results.